$TAS^+(Z)$-Me_3CNSN^- and $TAS^+(E)$-Me_3SiNSN^-: Does the Anion−Cation Interaction Influence the Configuration?

Tobias Borrmann,[†] Andrey V. Zibarev,[‡] Enno Lork,[‡] Gerd Knitter,[‡] Shan-Jia Chen,[‡] Paul G. Watson,[‡] Edgardo Cutin,[§] Makhmut M. Shakirov,[‡] Wolf-Dieter Stohrer,*[,†] and Rüdiger Mews*[,‡]

Institute of Organic Chemistry, University of Bremen, Postfach 33 04 40, 28334 Bremen, Germany, Institute of Inorganic and Physical Chemistry, University of Bremen, Postfach 33 04 40, 28334 Bremen, Germany, Institute of Organic Chemistry, Russian Academy of Sciences, Siberian Division, 630090 Novosibirsk, Russia, and Facultad de Bioquimica, Quimica y Farmacia, Instituto de Quimica Fisica, Universidad Nacional de Tucuman, Ayacucho 491, 4000 Tucuman, Argentina

Received April 10, 2000

TAS^+ salts (TAS = $(Me_2N)_3S$) of the sulfur diimide anions Me_3XNSN^- (X = C (**1a**), Si (**1b**)) were prepared by Si−N bond cleavage from the corresponding sulfur diimides $Me_3XNSNSiMe_3$ and TAS-fluoride ($(Me_2N)_3S^+Me_3SiF_2^-$) and characterized by X-ray crystallography and multinuclear NMR spectroscopy. According to the experimentally determined bond lengths and theoretical calculations, the Me_3XNSN^- anions are best described as thiazylamides $Me_3X-N-S\equiv N$ rather than sulfur diimides $Me_3X-N=S=N$. In agreement with the calculated and experimentally determined structures of the isoelectronic thionylimides RNSO, **1a** adopts the *Z*-configuration, which is electronically favored due to anomeric effects. The electronically disfavored *E*-configuration of **1b** in the solid state can be explained by weak anion−cation interaction.

Introduction

Alkali metal sulfur diimide salts K^+RNSN^- (R = Me_3C, Me_3Si)[1] and $Cs^+Me_3SiNSN^-$ [2] have been prepared by Si−N bond cleavage from the appropriate silyl derivatives $RNSNSiMe_3$, KNH_2, $KOCMe_3$, and CsF, respectively; phosphino, arsino, and sulfonyl derivatives (R = $(Me_3C)_2P$, $(Me_3C)_2As$, $PhSO_2$)[3,4] were obtained under similar conditions via N bond cleavage from the corresponding symmetric sulfur diimides RNSNR. $Li^+Me_3SnNSN^-$ was isolated from the reaction of $Me_3SnNSNSnMe_3$ with LiMe.[5] Under more drastic conditions, even the dianion is accessible as K_2N_2S[6] from the bis(silylated) derivative $Me_3SiNSNSiMe_3$ or from $KOCMe_3$ (molar ratio 1:2). The latter compound was first reported but poorly characterized from the reaction of KNH_2 with S_4N_4 (with "KNS" as a byproduct) or $(NSCl)_3$.[7]

These salts are very suitable for the transfer of $RNSN^-$ or N_2S^{2-} units in heterogeneous reactions.[8,9] Due to strong anion−cation interactions, they are almost insoluble in common aprotic solvents; therefore, structure determinations are unknown.

Recently, we have shown that arylsulfur diimide anions $ArNSN^-$ are readily accessible[10] by Si−N bond cleavage from the appropriate N−silyl−N′−aryl sulfur diimides $Me_3SiNSNAr$ and TAS-fluoride $(Me_2N)_3S^+Me_3SiF_2^-$. Similar to its isoelectronic counterpart the thionylimides RNSO, the Ar substituent is found exclusively in the *Z*-position in the $ArNSN^-$ anions.

Salts $TAS^+Me_3CNSN^-$ (**1a**) and $TAS^+Me_3SiNSN^-$ (**1b**) were reported simultaneous with our investigations[11] by the group of Herberhold.[12] They described the formation of these compounds from the corresponding potassium salts and TASF in a 1,2-dimethoxyethane/CH_3CN solution at room temperature after reaction over 2 days. The salts were characterized only by ^{14}N and ^{29}Si NMR spectroscopy in solution, and according to the spectra reported, product mixtures were obtained. This is expected, as TASF is known to react with CH_3CN under these conditions. Our attempts to recrystallize $TAS^+Me_3CNSN^-$ at room temperature from CH_3CN/ether over a period of several days led to the decomposition of the product with formation of $TAS^+S_3N_3^-$ and unidentified products.[11] As a result of the interpretation of the ^{14}N NMR spectra and on the basis of the calculated (GIAO) nitrogen-shielding constants, both anions were reported to adopt the *Z*-configuration in solution.[12]

* Corresponding author. Phone: + 49 421-218 3354. Fax: +49 421-218 4267. E-mail: mews@chemie.uni-bremen.de.
† University of Bremen.
‡ Russian Academy of Sciences.
§ Instituto de Quimica Fisica, Universidad Nacional de Tucuman.

(1) Hänssgen, D.; Ross, B. *Z. Anorg. Allg. Chem.* **1981**, *473*, 80.
(2) Haas, A.; Fleischer, U.; Mätschke, M.; Staemmler, V. *Z. Anorg. Allg. Chem.* **1999**, *625*, 681.
(3) Herberhold, M.; Ehrenreich, W.; Bühlmeyer, W.; Guldner, K. *Chem. Ber.* **1986**, *119*, 1424.
(4) Roesky, H. W.; Schmieder, W.; Sheldrick, W. S. *J. Chem. Soc., Chem. Commun*. **1981**, 1013. Roesky, H. W.; Schmieder, W.; Isenberg, W.; Sheldrick, W. S.; Sheldrick, G. M. *Chem. Ber.* **1982**, *115*, 2714.
(5) Hänssgen, D.; Steffens, R. *J. Organomet. Chem*. **1982**, *236*, 53.
(6) Herberhold, M.; Ehrenreich, W. *Angew. Chem.* **1982**, *94*, 637; *Angew. Chem., Int. Ed. Engl*. **1986**, *21*, 633.
(7) Berg, W.; Goehring, M. *Z. Anorg. Allg. Chem*. **1954**, *275*, 273.
(8) Herberhold, M.; Gerstmann, S.; Wrackmeyer, B. *Phosphorus, Sulfur Silicon Relat. Elem*. **1992**, *66*, 273.
(9) Herberhold, M.; Gerstmann, S.; Wrackmeyer, B. *Phosphorus, Sulfur Silicon Relat. Elem*. **1996**, *113*, 89, and references therein.
(10) Zibarev, A. V.; Lork, E.; Mews, R. *J. Chem. Soc., Chem. Commun*. **1998**, 991.
(11) Mews, R. In *Inorganic Fluorine Chemistry: Toward the 21st Century*; Thrasher, J. S., Strauss S. H., Edss; ACS Symposium Series 555; American Chemical Society: Washington, DC, 1994; p 148 (ref 55). Knitter, G. Ph.D. Thesis, University of Bremen, Bremen, Germany, 1994.
(12) Wrackmeyer, B.; Gerstmann, S.; Herberhold, M.; Webb, G. A.; Kurosu, H. *Magn. Reson. Chem.* **1994**, *32*, 492.

10.1021/ic0004030 CCC: $19.00
Published on Web 08/17/2000

Table 1. NMR Data of $TAS^+Me_3CN(2)SN(1)^-$ (**1a**) and $TAS^+Me_3SiN(2)SN(1)^-$ (**1b**)

	$^1H\delta$ (ppm)		$^{13}C\delta$ (ppm)		$^{14}N\delta$ (ppm)		$^{15}N\delta$ (ppm)		$^{29}Si\delta$ (ppm)	
R	solution	solid state	solution	solid state	solution	solid state	solution	solid state	solution	solid state
Me_3C	2.78(TAS^+)	3.62(TAS^+)	58.80($Me_3\underline{C}$)	55.78($Me_3\underline{C}$)	110(N(1))	no	107(N(1))	no		
	1.19(Me_3C)	1.77(Me_3C)	38.38(TAS^+)	38.37(TAS^+)	−72(N(2))	no	−75(N(2))	no		
			31.06($\underline{Me}_3C$)	31.58($\underline{Me}_3C$)	−321(TAS^+)	no	−325(TAS^+)	no		
Me_3Si	2.77(TAS^+)	3.57(TAS^+)	38.49($\underline{TAS}^+$)	38.19($\underline{TAS}^+$)	173(N(1))	no	170(N(1))	no	−15.3	−15.6
	−0.15(Me_3Si)	0.50(Me_3Si)	3.05(Me_3Si)	3.49(Me_3Si)	−94(N(2))	no	−98(N(2))	no		
					−331(TAS^+)	no	−325(TAS^+)	−324		

In the present paper, we report on the preparation and isolation of $TAS^+Me_3CNSN^-$ and $TAS^+Me_3SiNSN^-$ and on their solid-state structures determined by X-ray diffraction. While for the Me_3CNSN^- anion the expected *Z*-configuration is observed, Me_3SiNSN^- surprisingly shows an *E*-configuration. We discuss the reasons for the unexpected a priori difference in geometries of the anions by means of ab initio model calculations, and we develop a bonding model for these anions.

Experimental Section

Materials and Methods. TASF,[13] $Me_3SiNSNCMe_3$,[14] and $Me_3SiNSNSiMe_3$[15] were prepared according to literature methods. Acetonitrile was treated with P_4O_{10} and freshly distilled prior to use. The solution NMR spectra were recorded with Bruker DPX 200 (^1H, ^{13}C), Bruker AM 360 NB (^{14}N), and Bruker DRX 500 (^1H, ^{13}C, ^{15}N, ^{29}Si) spectrometers, and the CP MAS solid-state NMR spectra were recorded with a Bruker MSL 400 (^1H, ^{13}C, ^{15}N, ^{29}Si) spectrometer. Chemical shifts are given with respect to Me_4Si (^1H, ^{13}C, ^{29}Si) and $MeNO_2$ (^{14}N, ^{15}N), and IR spectra (Nujol mulls) were recorded on a Nicolet DX-55-FT-IR spectrometer. Elemental analyses were performed at Mikroanalytisches Labor Beller, Göttingen, Germany.

Preparation of $TAS^+Me_3CNSN^-$ (1a). TASF (1.27 g, 4.6 mmol) is placed in one side of a two-arm lambda-shaped glass vessel fitted with a Teflon valve. In this apparatus, 4.7 mmol (0.90 g) of $Me_3SiNSNCMe_3$ and 10 mL of CH_3CN are distilled via a vacuum line at −196 °C. The mixture is allowed to warm to −30 °C, and it is stirred at this temperature for 2 h. Complex **1a** is precipitated from this solution by the addition of 30 mL of ether (condensation via a vacuum line). The solvent mixture is decanted from the solid into the second arm of the vessel. After removal of all volatiles under vacuum, 1.25 g of **1a** (98%) is isolated as an orange-yellow solid. Table 1 lists the NMR data. IR (Nujol): 1354 (vs), 1272 (s), 1288 (s), 1175 (s), 1062 (m), 1036 (s), 1018 (m), 941 (vs), 905 (vs), 817 (s), 784 (m), 719 (vs), 694 (s), 669 (m), 644 (m), 613 cm^{-1} (m).

Anal. Calcd for $C_{10}H_{27}N_5S_2$ (281.49): C, 42.7; H, 9.7; S, 22.8. Found: C, 40.5; H, 9.5; S, 22.9.

Preparation of $TAS^+Me_3SiNSN^-$ (1b). Similar to **1a**, **1b** is prepared from $Me_3SiNSNSiMe_3$ and TASF, yielding an orange-yellow solid. See Table 1 for NMR data. IR (Nujol): 1282 (m), 1234 (m), 1190 (s, br), 1147 (w), 1040 (vs, br), 955 (vs), 935 (s), 905 (s), 845 (sh), 820 (s), 743 (m), 707 (m), 668 (m), 599 cm^{-1} (w).

Anal. Calcd for $C_9H_{27}N_5S_2Si$ (297.58): C, 36.3; H, 9.1; N, 23.5. Found: C, 36.1; H, 9.0; N, 23.3.

Computational Methods. All ab initio calculations were performed on an IBM-RS 6000 computer operating under the AIX 3.1 system with the GAUSSIAN 94 program.[16] Visualization of the electrostatic potential was conducted with the Hyperchem 5.01[17] program on a PC.

Crystallographic Analyses of 1a and 1b. Single crystals suitable for X-ray analyses were obtained by slow diffusion of ether into solutions of salts **1a** and **1b** in CH_3CN at −40 °C.

Complex 1a. The transparent orange-yellow crystal was mounted using KEL-F oil onto a thin glass fiber. Data were collected on a Siemens P4 four-cycle diffractometer using a graphite-monochromated MoKα beam (0.71073 Å). Of 4333 reflections collected with $\omega/2\theta$ scans for θ ranging from 2.73° to 27.49°, 3275 were independent, with $R_{int} = 0.0244$ after the usual Lorentztian and polarization correction. Details of the data collection and refinement are given in Table 2.

Table 2. Crystal Data and Structure Refinement for **1a** and **1b**

	1a	**1b**
empirical formula	$C_{10}H_{27}N_5S_2$	$C_9H_{27}N_5S_2Si$
mol wt	281.49	297.57
temp	173(2) K	173(2) K
wavelength	71.073 pm	71.073 pm
cryst syst, space group	triclinic, $P\bar{1}$	orthorhombic, *Pnma*
unit cell dimensions	$a = 638.1(5)$ pm	$a = 2121.6(2)$ pm
	$b = 1146.2(2)$ pm	$b = 1108.9(10)$ pm
	$c = 1156.9(2)$ pm	$c = 728.7(10)$ pm
	$\alpha = 95.88(1)°$	$\alpha = 90°$
	$\beta = 99.22(2)°$	$\beta = 90°$
	$\gamma = 100.85(2)°$	$\gamma = 90°$
V	0.8126(7) nm^3	1.7144(3) nm^3
Z	2, 1.150 Mg/m^3	4, 1.153 Mg/m^3
absorption coefficient	0.318 mm^{-1}	0.372 mm^{-1}
F(000)	308	648
cryst size	$1.0 \times 0.6 \times 0.6$ mm^3	$0.7 \times 0.6 \times 0.6$ mm^3
θ range for data collection	2.73−27.49°	2.66−27.48°
index ranges	$-8 \le h \le 1, -14 \le k \le 14, -15 \le l \le 15$	$-11 \le h \le 27, -14 \le k \le -1, -1 \le l \le 9$
reflections collected/unique	4333/3275 (R_{int} = 0.0244)	2803/2069 (R_{int} = 0.0348)
refinement method	full-matrix least-squares on F^2	full-matrix least-squares on F^2
data/restraints/parameters	3275/0/165	2069/0/101
goodness-of-fit on F^2	1.033	0.978
final *R* indices[a]	R1 = 0.0315, wR2 = 0.0860	R1 = 0.0347, wR2 = 0.0920
R indices (all data)	R1 = 0.0351, wR2 = 0.0891	R1 = 0.0477, wR2 = 0.0957
extinction coefficient	0.035(4)	0.0084(13)
largest diff. peak and hole	282 and −317 e nm^{-3}	211 and −351 e nm^{-3}

[a] $wR2 = \{\Sigma[w(F_o^2 - F_c^2)^2]/\Sigma[w(F_o^2)^2]\}^{1/2}$. $R1 = \Sigma||F_o| - |F_c||/\Sigma|F_o|$.

Complex 1b. Of the 2803 reflections collected with $\omega/2\theta$ scans for θ ranging from 2.66° to 27.48°, 2069 were independent, with $R_{int} = 0.0348$ after the usual Lorentztian and polarization correction. Details of the data collection and refinement are given also in Table 2.

The structure was solved by direct methods (SHELXS[18]). Subsequent least-squares refinements (SHELXL 97-2)[18] located the positions of the remaining atoms in the electron density maps. All non-H atoms were refined anisotropically.

(13) Middleton, W. J. *Org. Synth*. **1985**, *64*, 221.
(14) Ruppert, I.; Bastian, V.; Appel, R. *Chem. Ber*. **1975**, *108*, 2329.
(15) Scherer, O. J.; Wies R. *Z. Naturforsch*. **1970**, *25b*, 1486.
(16) Frisch, M. J.; Trucks, G. W.; Schlegel, H. B.; Gill, P. M. W.; Johnson, B. G.; Robb, M. A.; Cheeseman, J. R.; Keith, T.; Petersson, G. A.; Montgomery, J. A.; Raghavachari, K.; Al-Laham, M. A.; Zakrzewski, V. G.; Ortiz, J. V.; Foresman, J. B.; Cioslowski, J.; Stefanov, B. B.; Nanayakkara, A.; Challacombe, M.; Peng, C. Y.; Ayala, P. Y.; Chen, W.; Wong, M. W.; Andres, J. L.; Replogle, E. S.; Gomerts, R.; Martin, R. L.; Fox, D. J.; Binkley, J. S.; Defrees, D. J.; Baker, J.; Stewart, J. P.; Head-Gordon, N.; Gonzalez, C.; Pople, J. A. *Gaussian 94*, Revision C.3; Gaussian: Pittsburgh, PA, 1995.
(17) *HyperChem Release 5.0 for Windows*; Hypercube, Inc.: Gainesville, FL, 1998.
(18) Sheldrick, G. M. *SHELX-97*; University of Göttingen: Göttingen, Germany, 1997.

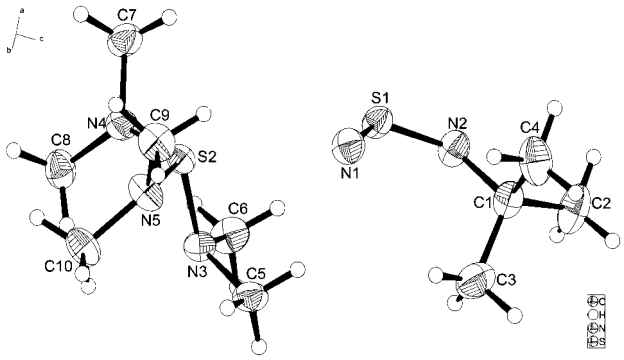

Figure 1. DIAMOND plot[23] of $TAS^+Me_3CNSN^-$ (**1a**) (50% probability ellipsoids). Selected bond lengths and angles: S(1)−N(1) 149.0(1) pm, S(1)−N(2) 157.6(1) pm, N(2)−C(1) 147.4(2) pm, N(1)−S(1)−N(2) 125.82(7)°, S(1)−N(2)−C(1) 123.81(10)°.

Scheme 1

$$Me_3SiNSNR + TASF \longrightarrow TAS^+RNSN^- + 2\,Me_3SiF$$

1a R=Me_3C, **1b** R = Me_3Si

Results

The reaction of N-silylated sulfur diimides with TASF $[(Me_2N)_3S]^+[Me_3SiF_2]^-$ [13] at −30 °C is a generally applicable approach to organic-solvent-soluble sulfur diimide salts under very mild conditions (see Scheme 1). Previous experiments have shown that this might be a general approach to alkyl- and arylsulfur diimide anions;[10] this method has been extended to heterosubstituted derivatives.[19]

Complex **1b** does not react with an excess of TASF to give the dianion N_2S^{2-}, and the negative charge in **1b** prevents the attack of another fluoride. But with better F^- donors—e.g., $Me_4N^+F^-$ [20,21]—even the second Si−N bond might be cleaved.[22]

Salts **1a** and **1b** are orange-yellow moisture-sensitive solids. They can be handled at room temperature but are stored preferably at −30 °C. Carefully prepared CH_3CN solutions are stable at −10 °C; at room temperature, slow decomposition occurs. Salts **1a** and **1b** were characterized by elemental analysis and IR and multinuclear NMR spectroscopy, as well as X-ray crystallography.

The results of ^1H, ^{13}C, and ^{29}Si NMR investigations of solutions, as well as CP MAS data of **1a** and **1b**, are listed in Table 1. ^{14}N and ^{15}N chemical shifts are also given for solutions. Attempts to obtain solid-state data for these nuclei were successful only for the TAS cation of **1b**. Our ^{14}N and ^{29}Si results for **1a** and **1b** agree reasonably well with those reported by Herberhold and co-workers; only the ^{14}N chemical shift of the terminal nitrogen of **1a** differs by more than 10 ppm.

The solid-state structures of the salts **1a** and **1b** are shown in Figure 1[23] and Figure 2,[23] and the details of the structure determination are listed in Table 2.

Complex **1a** shows the expected *Z*-configuration, while for **1b** the *E*-configuration is found in contrast to the calculations and the interpretation of ^{14}N NMR investigations in solution.[12] Any explanation for the different configurations of **1a** and **1b**

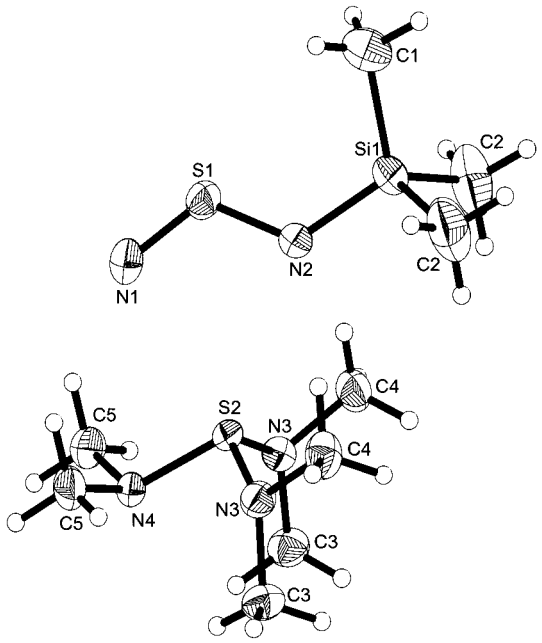

Figure 2. DIAMOND plot[23] of $TAS^+Me_3SiNSN^-$ (**1b**) (50% probability ellipsoids). Selected bond lengths and angles: S(1)−N(1) 146.7(2) pm, S(1)−N(2) 156.4(3) pm, N(2)−Si(1) 171.7(3) pm, N(1)−S(1)−N(2) 121.3(2)°, S(1)−N(2)−Si(1) 124.5(2)°.

cannot be derived from different reaction mechanisms of their formation. Calculations for $Me_3CNSNSiMe_3$[24] are in accordance with NMR investigations;[8] the most stable configuration is (*E*)-Me_3Si−NSN−(*Z*)-CMe_3. The primary product of reaction 1 should be the observed (*Z*) Me_3CNSN^-. X-ray investigations of $Me_3SiNSNSiMe_3$ uncovered an *E*/*Z*-configuration,[25,26] and NMR investigations in solution deduced rapid *E*/*Z* exchange.[25,27,28] Complex **1b** in the *E*-configuration might be possible as the primary product, but its isomerization to the more stable (according to the calculations) *Z*-configuration is not hindered by a high barrier of activation.[29]

The anions of salt **1** should be described as thiazylamides **A** rather than as sulfur diimide ions **B**, as the experimentally determined bond lengths indicate (Scheme 2). The RHF-calculated bond lengths are in slightly better agreement with these experimental values than are the MP2 results (Table 3).

The calculated dihedral angles between the CMe_3 or $SiMe_3$ groups and the N(2)−S(1) bond differ by 60° from the values found in the crystal structure determinations. Thus, the structures were optimized again for a better comparison, and the dihedral angles were kept at their measurements in the crystal due to intermolecular interaction (see below). The rotation of these terminal groups has, as expected, practically no influence on

(19) $TAS^+FSO_2NSN^-$ was obtained through this method: Niyogi, D.; Mews, R. Results to be published.
(20) Christe, K. O.; Wilson, W. W.; Wilson, R. D.; Bau, R.; Feng, J. *J. Am. Chem. Soc.* **1990**, *112*, 7619.
(21) Kolomeitsev, A. A.; Seifert, F. U.; Röschenthaler, G. V. *J. Fluorine Chem.* **1995**, *71*, 47.
(22) Watson, P. G.; Mews, R. Unpublished observations.
(23) *DIAMOND − Visual Crystal Structure Information System*; Crystal Impact: Bonn, Germany, 1999.
(24) RHF/6-31+G* energy of (*E*)-$SiMe_3$−NSN−(*Z*)-CMe_3 is −1070.8622 au and (*Z*)-$SiMe_3$−NSN−(*E*)-CMe_3 is −1070.8605 au, ΔE = 4.5 kJ/mol.
(25) The distances from the solid-state structure of $Me_3SiNSNSiMe_3$ to the *E*-fragment and the *Z*-fragment are slightly shorter (151.55(6) pm), as expected. See: Herberhold, M.; Gerstmann, S.; Wrackmeyer, B.; Borrmann, H. *J. Chem. Soc., Dalton Trans*. **1994**, 633.
(26) In the gas phase, $Me_3SiNSNSiMe_3$ exists in a distorted *Z*-configuration with an S−N distance of 153.6(3) pm. See: Anderson, D. G.; Robertson, H. E.; Rankin, D. W. H.; Woollins, J. D. *J. Chem. Soc., Dalton Trans.* **1989**, 859.
(27) Belton, P. S.; Woollins, J. D. *Magn. Reson. Chem*. **1986**, *24*, 1080.
(28) Chivers, T.; Oakley, R. T.; Scherer, O. J.; Wolmershäuser, G. *Inorg. Chem*. **1981**, *20*, 914.
(29) RHF/6-31+G* optimized transition state (NIMAG = 1, −82.0 cm^{-1}) from the *E*- to the *Z*-configuration of Me_3SiNSN^-: −914.1466 au, α_{SNSi} = 142.7°, τ_{NSNSi} = 114.4° (in comparison, (*E*)-Me_3SiNSN^- = −914.1480 au and (*Z*)-Me_3SiNSN^- = −914.1545 au).

Table 3. RHF/6-31+G* and MP2/6-31+G* Calculated and Experimental Bond Lengths and Angles for **1a** and **1b**

		N(1)−S(1) (pm)	S(1)−N(2) (pm)	N(2)−R (pm)	N(1)−S(1)−N(2) (deg)	S(1)−N(2)−R (deg)
	RHF	147.4	157.4	145.2	124.97	125.35
Z-Me_3CNSN^-	MP2	152.2	161.2	147.4	125.56	122.02
	exp.	149.0(1)	157.6(1)	147.4(2)	125.82(7)	123.81(10)
	RHF	146.7	157.1	167.2	119.51	133.38
E-Me_3SiNSN^-	MP2	150.0	160.9	172.1	121.96	124.10
	exp.	146.7(2)	156.4(3)	171.7(3)	121.3(2)	124.5(2)

Scheme 2

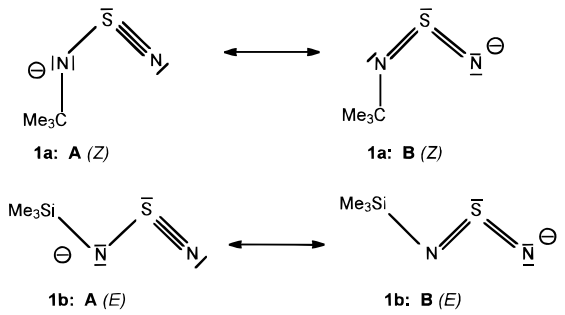

Table 4. RHF and MP2 Calculated Energies and Energy Differences of (*E*)- and (*Z*)-RNSO

(a) (*E*)- and (*Z*)-RNSO

RNSO		ΔE, *E*−*Z* (kJ/mol)	energy (au) *E*	energy (au) *Z*	NIMAG *E*	NIMAG *Z*
HNSO	RHF	19.7	−527.3189	−527.3264	0	0
	MP2	20.8	−527.8199	−527.8278	−	−
Me_3CNSO	RHF	24.2	−683.4608	−683.4700	0	0
	MP2	28.9	−684.5007	−684.5117	−	−
F_3CNSO	RHF	14.7	−862.9442	−862.9498	0	0
	MP2	19.4	−864.0919	−864.0993	−	−
Me_3SiNSO	RHF	17.3	−934.5773	−934.5839	0	0
	MP2	21.5	−935.5598	−935.5680	−	−
F_3SiNSO	RHF	10.2	−1114.2372	−1114.2411	0	0
	MP2	13.1	−1115.3428	−1115.3478	−	−

(b) (*E*)- and (*Z*)-$RNSN^-$

$RNSN^-$		ΔE, *E*−*Z* (kJ/mol)	energy (au) *E*	energy (au) *Z*	NIMAG *E*	NIMAG *Z*
$HNSN^-$	RHF	21.3	−506.8839	−506.8920	0	0
	MP2	23.4	−507.3785	−507.3874	−	−
Me_3CNSN^-	RHF	31.0	−663.0155	−663.0273	1	0
	MP2	36.0	−664.0529	−664.0666	−	−
	RHF	26.8	−663.0171	0		
	MP2	36.3	−664.0528	−	−	
F_3CNSN^-	RHF	12.3	−842.5545	−842.5592	1	0
	MP2	10.0	−843.6905	−843.6943	−	−
	RHF	4.4	−842.5575	0		
	MP2	5.8	−843.6921	−	−	
Me_3SiNSN^-	RHF	17.1	−914.1480	−914.1545	1	0
	MP2	21.5	−915.1204	−915.1286	−	−
	RHF	16.6	−914.1482	0		
	MP2	22.9	−915.1199	−	−	
F_3SiNSN^-	RHF	7.1	−1093.8503	−1093.8530	1	0
	MP2	8.1	−1094.9414	−1094.9445	−	−
	RHF	7.1	−1093.8503	0		
	MP2	9.7	−1094.9408	−	−	

the bond lengths reported in Table 3 and only a slight influence on the energy, as shown in Table 4b.

The distance between the sulfur and the terminal nitrogen (d_{S1N1} = 146.7(2) pm) is in the range of the $S^{IV}{\equiv}N$ triple bond distance; the RN(2)−S(1) bond length in **1b** ($d_{S(1)N(2)}$ = 156.4(3) pm) is slightly longer than in the parent sulfur diimide RN═S═NR (152.3(1) pm)[25] and the isoelectronic thionylimide RN═S═O (150.8(5) pm)[30] (R = Me_3Si). For **1a**, significantly longer bond distances are found for S1−N1 ($d_{S(1)N(1)}$ = 149.0(1) pm) as well as for S(1)−N(2) (d_{S1N2} = 157.6(1) pm) compared to those of **1b**.

Discussion

Three aspects in this paper are of special interest: the unexpected *E*-configuration of the Me_3Si derivative, the influence of the terminal CMe_3 group(s) compared to the $SiMe_3$ group(s), and the bonding description of these anions as thiazylamides.

Thionylimides RNSO are isoelectronic with the anions of salt **1**. According to structural investigations, they are present exclusively as *Z*-isomers.[31] Even with sterically demanding groups (e.g., Me_3Si[30]), it is not possible to force the substituent into the more favorable *E*-position. According to our MP2 calculations, the *Z*-isomers are more stable by 13−29 kJ/mol compared to the *E*-isomers of the examples given in Table 4a. Similar results are obtained for the sulfur diimide (thiazylamide) ions (cf. Table 4b), where all examples show the *Z*-isomers to be more stable.

There are three stereoelectronic factors favoring the sterically a priori disfavored *Z*-configuration (Scheme 3): (i) the destabilizing interaction between the two occupied nonbonding $n_{N(2)}$ and $n_{S(1)}$ orbitals is less pronounced in the *Z*-configuration, where these two orbitals are synplanar, compared to the *E*-configuration, where the two orbitals are antiplanar (Scheme 3a); (ii) the stabilizing anomeric interaction[32] between the occupied $n_{N(2)}$ orbital and the unoccupied $\sigma^*_{S(1)-N(1)}$ orbital is only significant in an antiplanar arrangement of these orbitals, as is the case in the *Z*-configuration (Scheme 3b); (iii) the same holds for the stabilizing anomeric interaction between the occupied $n_{S(1)}$ orbital and the unoccupied $\sigma^*_{N(2)-R}$ orbital (Scheme 3c).

The last anomeric effect should increase with increasing acceptor strength of the $\sigma^*_{N(2)-R}$ orbital, thus stabilizing the *Z*-configuration even more compared to the *E*-configuration. The calculations in Table 4, however, indicate the opposite.

The reason is the following: there is also a significant inverse hyperconjugation[32] between the nonbonding $n_{N(2)}$ orbital and the σ^* orbitals of the C−C (**1a**) and Si−C (**1b**) bonds, respectively, of the XMe_3 group. The electronic factors for this inverse hyperconjugation do not differ in the two configurations under discussion (Scheme 3d). However, the stronger this negative hyperconjugation is, the less electron density remains localized in the $n_{N(2)}$ orbital, thus decreasing the first and second aforementioned factors. This, in turn, results in a relative decrease in the stability of the electronically favored but sterically disfavored *Z*-configuration, as confirmed by the calculations for the as yet unknown model compounds with CF_3 or SiF_3 as terminal groups. These strong electron-withdrawing groups do reduce the calculated energy differences between the

(30) *Gmelin Handbook of Inorganic and Organometallic Chemistry, Sulfur Nitrogen Compounds*, Part 6; Springer-Verlag, Berlin, 1990; p 4ff.
(31) Gobbato, K. I.; Della Vedova, C. O.; Oberhammer, H. *J. Mol. Struct.* **1995**, *350*, 227.
(32) Reed, A. E.; Schleyer, P. v. R. *Inorg. Chem.* **1988**, *27*, 3969, and references therein.

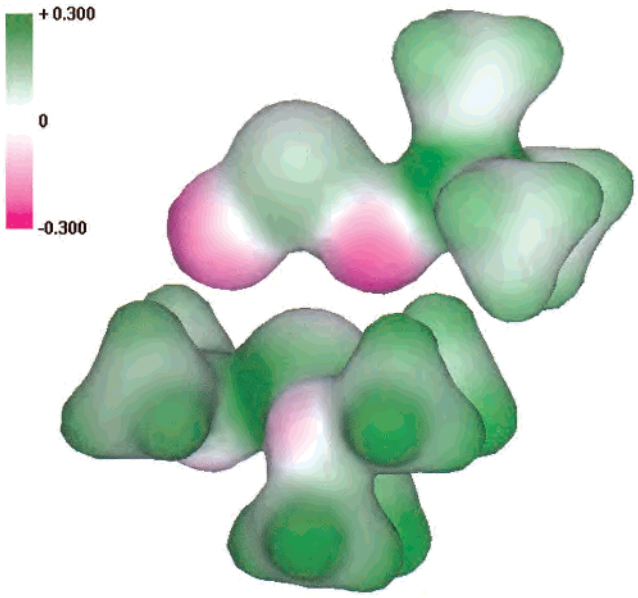

Figure 3. PM3-calculated electrostatic potential of the ion pair (*E*)-$Me_3SiNSN^-TAS^+$ projected on the isoelectron density surface.[15]

Scheme 3

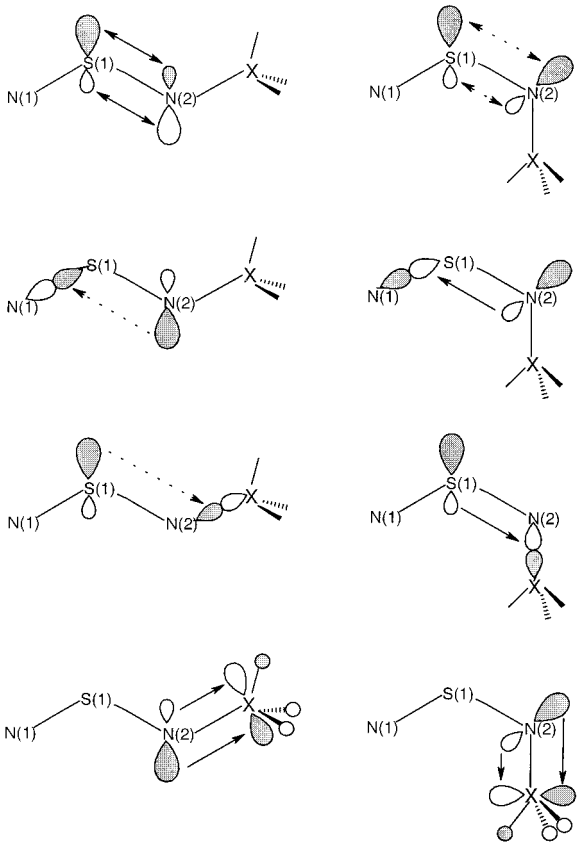

E- and the *Z*-configurations, but even they are unable to reverse the relative stabilities of the *E*- and the *Z*-configurations. So the observation of the unexpected *E*-configuration for the silyl derivative **1b** in the solid state must be due to factors other than stereoelectronic ones.

Figure 3 shows the PM3-calculated electrostatic potential of the ion pair TAS$^+$(*E*)-Me_3SiNSN^- (**1b**) projected onto the isoelectron density surface. It clearly demonstrates that the Me_3SiNSN^- anion is not "naked" and that the *E*-configuration is ideally suitable for electrostatic interactions between anion and cation. A similar interaction and stabilization of the *E*-configuration is expected for TAS$^+Me_3CNSN^-$ (**1a**). We believe that the reason for the formation of the *E*-configuration in **1b** (and not in **1a**) is the smaller energy difference between the *E*/*Z*-isomers. In the silyl salt **1b** but not in the *tert*-butyl salt **1a**, this energy difference is overcompensated by the Coulombic interaction between anion and cation.

From NMR investigations in solution, it was concluded that both ions, Me_3CNSN^- and Me_3SiNSN^-, adopt the electronically and computationally favored *Z*-configuration under these conditions. This assumption was supported by relating the experimental results to calculated GIAO shielding constants.[12]

From multinuclear NMR solution and CP MAS experiments, we expected to confirm the different configurations of Me_3SiNSN^- in solution and solid state. Unfortunately, it was only possible to obtain ^{1}H, ^{13}C, and ^{29}Si data. For the silyl salt, an additional ^{14}N signal for the TAS$^+$ cation at -324 ppm was obtained, in excellent agreement with $\delta_N = -324.2$ ppm in solution. From our GIAO calculations on the RHF/6-31+G* level of theory for Me_3SiNSN^- and Me_3CNSN^-, no significant difference in the ^{1}H, ^{13}C, and ^{29}Si chemical shifts for the respective *E*- and *Z*-configurations is expected. Comparison of solution and solid-state CP MAS NMR data therefore allows no conclusions to be made on the configurations present.

From our calculations for (*E*) and (*Z*)-Me_3SiNSN^-, we expect a chemical shift difference of $\Delta(\delta N) \approx 1$ ppm for the terminal nitrogen N(1) and $\Delta(\delta N) \approx 10$ ppm for the bridging nitrogen N(2). The data reported by Herberhold for the latter nitrogen are -96 and -94 ppm for TAS$^+Me_3SiNSN^-$ and $(Me_3C)_4N^+$-Me_3SiNSN^-, respectively. We obtained -94 and -98 ppm for TAS$^+Me_3SiNSN^-$ from ^{14}N and ^{15}N NMR and -93 ppm (^{14}N) for $Me_4N^+Me_3SiNSN^-$. The small differences in the chemical shifts suggest that the configuration in solution is independent of the counterion. Because the tetraalkylammonium salts are not suitable for the previously described Coulombic interaction, the *Z*-configuration might be present in solution. However, due to the small differences of $\Delta(\delta N)$ calculated for the bridging nitrogen in (*E*/*Z*)-Me_3SiNSN^-, this conclusion is not fully beyond any doubt. Attempts to obtain single crystals suitable for X-ray structure investigations of $Me_4N^+Me_3SiNSN^-$, where the anion should have the *Z*-configuration, have been unsuccessful to date.

A second interesting aspect results from the replacement of X = C by X = Si in the sulfur diimides and the thiazylamide ions. Both the nitrogen−sulfur bond lengths are reduced; the $S-N_E$ bond, however, is significantly stronger than the $S-N_Z$ bond, as shown in Scheme 4a.

This can be easily understood in a qualitative manner: Due to the (stronger) inverse hyperconjugation of the $SiMe_3$ group as compared with the CMe_3 group, the electron density in both the n_E and n_Z orbitals is reduced when C is replaced with Si. This reduction of electron density influences both the S−N bonds: (i) the strong repulsion between the two antiperiplanar orbitals n_S and n_E is reduced, thus shortening the $S-N_E$ bond significantly (abbreviated qualitatively in Scheme 4 as "ss"). (ii) The less pronounced repulsion between the two synperiplanar orbitals n_S and n_Z is reduced too, thus shortening the $S-N_Z$ bond as well, though to a lower excess (abbreviated as "s"). (iii) The anomeric interaction $n_Z \rightarrow \sigma^*_{S-N_E}$ is reduced, thus lengthening the $S-N_Z$ bond (abbreviated as "l") and shortening the $S-N_E$ bond (abbreviated as "s"). (iv) The anomeric interaction $n_S \rightarrow \sigma^*_{N_Z-Si}$ is increased compared with the less accepting $\sigma^*_{N_Z-C}$ orbitals (as model calculations clearly confirm), thus decreasing the bond length $S-N_Z$.

Scheme 4

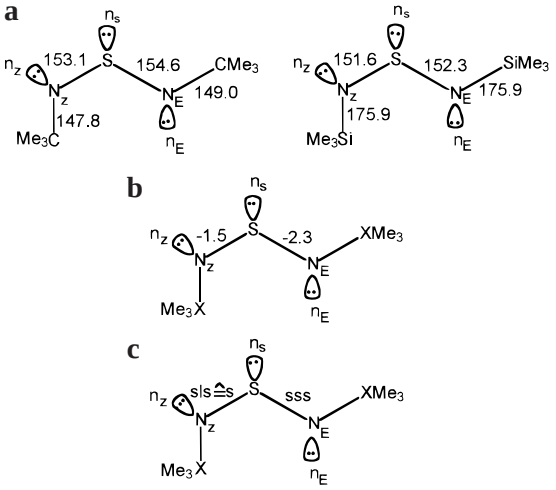

Scheme 5

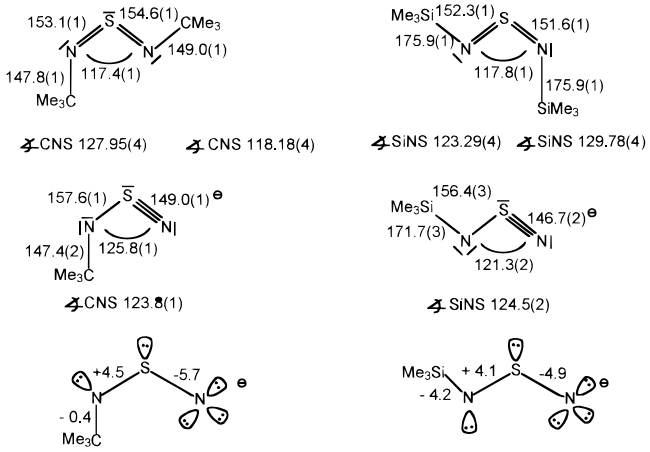

The addition of these fairly qualitative factors (Scheme 4c) indicates in fact a stronger reduction (sss) of the S−N_E bond length as compared to the weaker reduction (s) of the S−N_Z bond length in accordance with the experimental results shown in Scheme 4a.

The third interesting aspect is the bonding description of these anions as thiazylamides and not as sulfur diimides. Scheme 5 shows the bond distances and angles of $Me_3CNSNCMe_3$,[33] $Me_3SiNSNSiMe_3$, [25] and their corresponding anions.

The formation of the anions results in both the CMe_3- and the $SiMe_3$-substituted species in an increase of the N(2)−S bond length and a decrease of the S−N(1) bond length; the C−N(2) bond length is kept constant, whereas the corresponding Si−N(2) bond length is drastically shortened upon the formation of the anion. Qualitative arguments again give the explanation for these changes in bond lengths: (i) MP2-FC/6-31+G* calculations for a simplified model (Scheme 6) show that, not unexpectedly, the calculated S−N bond length depends closely on the S−N−R angle, i.e., on the hybridization of N. In the forced linear arrangement, this bond is found to be identical in length to that in the anion and significantly shorter than in the stable bent conformation.

Thus, the sharp decrease of the S−N(1) bond length upon the formation of the anion is not the result of the increased charge density on N(1) but simply of the change in hybridization from sp^2 to sp on this atom, which is well known to increase

Scheme 6

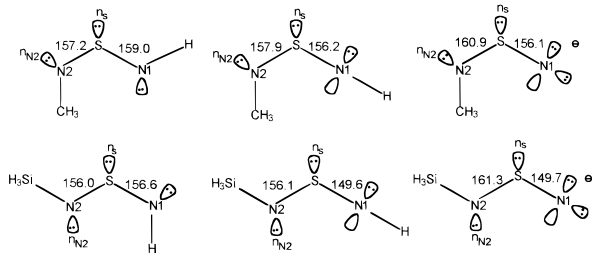

the bond strength. (ii) The experimentally found and calculation-confirmed increase of the N(2)−S bond length is, however, not the result of different hybridization of N1 but, rather, of the increase in electron density on N1 and the accompanying rise in energy of the lone−occupied orbitals on N1, by which the anomeric interaction between these orbitals and the empty $\sigma^*_{N(2)-S}$ orbital is increased so that this bond is lengthened. (iii) The expected accompanying shortening of the S−N(1) bond is compensated by the increase in repulsion between the lone occupied orbitals of N(1) and the lone n_S orbital. (iv) The negative charge also raises the energy of the lone occupied $n_{(N)2}$ orbital, which results in an increase of the anomeric interaction between the $n_{N(2)}$ and the σ^* orbitals of $SiMe_3$, which is the origin of the observed and calculated shortening of the Si−N(2) bond. The CMe_3 group does not show a comparable acceptor strength, so the C−N(2) bond is not influenced by the formation of the anion.

Conclusion

The TAS^+ cation $(Me_2N)_3S^+$ was thought to be an ideal counterion for the generation of naked anions. This might be true in solution, but the present study and other reports from our group[34,35] have shown that in the solid state, the sulfonium centers might undergo weak but definite Coulombic interactions with the counteranions. We believe that for the present case, this interaction is responsible for the formation of the stereoelectronically disfavored *E*-configuration in the Me_3SiNSN^- anion. If our conclusions are correct, then in the absence of such interactions (e.g., with cations such as $TAOS^+$, $(Me_2N)_3SO^+$,[35] Me_4N^+, Ph_4P^+, etc.), Me_3SiNSN^- should also adopt the *Z*-configuration in the solid state. On the other hand, the increasing interaction (e.g., with $(CF_3S(NMe_2)_2)^{+36}$ as counterion) could favor the *E*-configuration even for the Me_3CNSN^- anion.

The ions R_3XNSN^- are best described as thiazylamide ions $R_3X-\underline{\overset{\ominus}{N}}-\bar{S}\equiv N|$. The strengthening of the terminal SN bond in the anions compared to the neutral sulfur diimides $Me_3X-N{=}S{=}N-XMe_3$ is due to a change in the hybridization at the terminal nitrogen from sp^2 to sp. The weakening of the bridging S−N bond results from an increased negative hyperconjugation. This bonding description seems to be more general; a similar change is observed in the $R-N{=}S{=}O/N\equiv S-\underline{\bar{O}}|^{\ominus}$ [30,31,37−39] and $RN{=}C{=}NR/R-\underline{\overset{\ominus}{N}}-C\equiv N|$ systems.[40−43]

(33) Herberhold, M.; Gerstmann, S.; Milius, W.; Wrackmeyer, B.; Bormann, H. *Phosphorus, Sulfur Silicon Relat. Elem.* **1996**, *112*, 261.

(34) Wessel, J.; Behrens, U.; Lork, E.; Mews, R. *Angew. Chem.* **1995**, *107*, 516; *Angew. Chem., Int. Ed. Engl.* **1995**, *34*, 443.

(35) Wessel, J. Ph.D. Dissertation, University of Bremen, Bremen, Germany, 1995. Wessel, J.; Lork, E.; Mews, R. Results to be published.

(36) Mews, R. ACS 14th Winter Fluorine Conference, Abstr. 18; St. Petersburg, FL, 1999. Viets, D.; Lork, E.; Müller, M.; Mews, R. Results to be published.

(37) NSO^- ab initio calculations. See: Ehrhardt, C.; Ahlrichs, R. *Chem. Phys.* **1986**, *108*, 417.

(38) So, S. P. *Inorg. Chem.* **1989**, *28*, 2888.

(39) $Me_4N^+NSO^-$, X-ray structure. See: Mann, S.; Jansen, M. *Z. Naturforsch.* **1994**, *49b*, 1503.

Acknowledgment. This work was supported in part by the Deutsche Forschungsgemeinschaft (436 RUS 113/486/1), the Russian Foundation of Basic Research (98-03-04107), and the DAAD. A. V. Z. thanks the Royal Society of Chemistry for the RSC Journals Grant for International Authors.

(40) $Me_3SiNCNSiMe_3$, X-ray structure. See: Obermeyer, A.; Kienzle, A.; Weidlein, J.; Riedel, R.; Simon, A. *Z. Anorg. Allg. Chem*. **1994**, *620*, 1357.
(41) Jansen, M.; Jüngermann, H. *Z. Kristallogr*. **1994**, *209*, 779.
(42) GED. See: Hammel, A.; Volden, H. V.; Haaland, A.; Weidlein, J.; Reischmann, R. *J. Organomet. Chem.* **1991**, *408*, 35.
(43) Compared to $Me_3SiNCNSiMe_3$ in $TAS^+Me_3SiNCN^-$, the terminal C−N bond is shortened by ∼4 pm, and the bridging N−C bond is lengthened by ∼8 pm. See: Müller, M. Diploma Thesis, University of Bremen, Bremen, Germany, 1999.

Supporting Information Available: Tables listing detailed crystalographic data, atomic positional parameters, and bond lengths and angles. Both structures are available as CCDC 101271. This material is available free of charge via the Internet at http://pubs.acs.org.

IC0004030